

# REVISITING THE LONGITUDINAL 90 DEGREE LIMIT FOR SUPERCONDUCTING LINEAR ACCELERATORS

Ingo Hofmann<sup>\*</sup>, <sup>1, 2</sup>, Technische Universität Darmstadt, Darmstadt, Germany

<sup>1</sup>also at GSI Helmholtzzentrum für Schwerionenforschung GmbH, Darmstadt, Germany

<sup>2</sup>also at Goethe Universität, Frankfurt am Main, Germany

## Abstract

In the design of high-intensity linear accelerators one of the generally adopted criteria is not to exceed a zero-current phase advance per focusing period of  $90^\circ$  in order to avoid the space charge driven envelope instability, or a coinciding fourth order space charge structure resonance. Recently it was claimed that in certain structures such a constraint is not always necessary in the longitudinal plane (I. Hofmann and O. Boine-Frankenheim, Phys. Rev. Lett. 118, 2017). In FODO focusing structures with an rf gap per drift, for example, the transverse focusing period only induces a very weak (negligible) space charge force in the longitudinal plane. Hence, the longitudinal  $90^\circ$  stopband is practically irrelevant and values of  $k_{0,z}$  - as usual defined per transverse focusing period - significantly above  $90^\circ$  are possible in such structures, which grants additional design freedom. It is also shown that the latter is theoretically limited by a novel type of instability, the coupled envelope “sum mode”, which can be avoided by observing  $k_{0,z} + k_{0,x,y} < 180^\circ$ . Application of this finding is primarily for superconducting linear accelerators with high accelerating gradients.

## INTRODUCTION

The existence of a stopband at  $90^\circ$  phase advance has resulted in the definition of a well-known design limit for high intensity accelerators. After numerous theoretical studies (see, for example, Ref. [1]) and an early transport experiment [2] the first experimental study confirming the existence of such a  $90^\circ$  stopband in the transverse plane for an operational high-current linac was reported in Ref. [3]. This experiment also gave evidence of a fourth order space charge structural resonance in this stopband rather than the traditionally expected envelope instability. For a detailed theoretical discussion of the competing effects of this fourth order structural resonance with the envelope instability in the common  $90^\circ$  stopband see Ref. [4]; further details of the correlation with the upper respectively lower edge of the stopband are discussed in Ref. [5].

The significance of the *transverse*  $90^\circ$  stopband as linac design limitation is unquestioned. However, a corresponding longitudinal stopband - traditionally assumed at  $k_{0,z} \approx 90^\circ$  - has been assumed as given. Recently the need for a re-examination of this assumed limit was suggested in Ref. [6] for FODO-type lattices with more than one rf gap per transverse focusing period.

## REVIEW OF THE LONGITUDINAL $90^\circ$ STOPBAND

We first review the  $90^\circ$  longitudinal stopband for a periodic solenoid lattice with an rf gap between solenoids (assuming, for simplicity, no acceleration), where the longitudinal cell definition coincides with the transverse one as shown in Fig. 1.

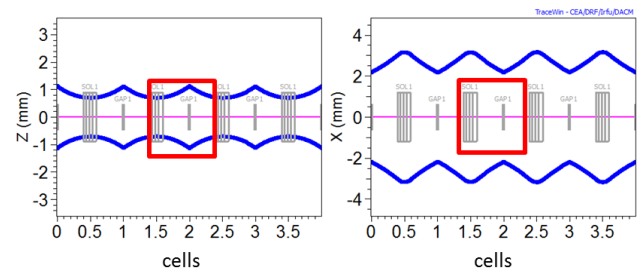


Figure 1: Layout of solenoid lattice example.

We use the TRACEWIN [7] code and assume an ellipsoidal bunch with equal emittances in  $x, y, z$  and Gaussian distribution (cut at  $3\sigma$ ) in a lattice with  $k_{0,z} = 120^\circ$  ( $k_{0,x,y} = 60^\circ$ ) and a space charge depressed  $k_z = 76^\circ$ . Results for the rms emittances and self-consistent phase advances are shown in Fig. 2. There is a clear evidence of the  $90^\circ$  longitudinal stopband due to the fact that the longitudinal period is identical to the transverse one.

As expected, there is a significant rms emittance growth, which resembles qualitatively the behaviour in the transverse stopband [4]. The rms emittances show an initial rise of about 40%, followed by a plateau and a second phase with large growth of over 200%. The phase space plots confirm that the initial rise is due to a fourth order space charge structure resonance, and - after a mode switch on the plateau - a following envelope instability. Note that the strong envelope instability also manifests itself in oscillations of the rms phase advance plotted in the centre graph of Fig. 2.

The complete stopband is shown in Fig. 3. For comparison we also show the stopband for  $k_{0,z} = 100^\circ$ , which is considerably smaller due to the lower current needed for resonance. Both stopbands start - similar to the transverse case - for  $k_z < 90^\circ$  and lead to significant rms emittance growth. Inspection of phase space plots allows to distinguish between two emittance growth regimes: the initial one up to the plateau, which is ascribed to the fourth order space charge resonance, followed by the envelope instability regime. It is thus possible to distinguish in Fig. 3 between growth attributed to the fourth order structure resonance and the total growth by the additional envelope instability

<sup>\*</sup> i.hofmann@gsi.de

Content from this work may be used under the terms of the CC BY 3.0 licence (© 2018). Any distribution of this work must maintain attribution to the author(s), title of the work, publisher, and DOI.

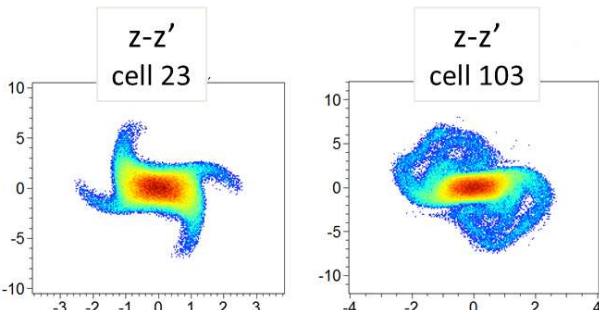
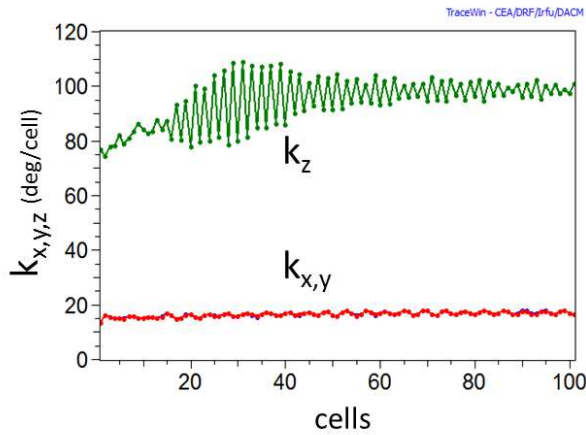
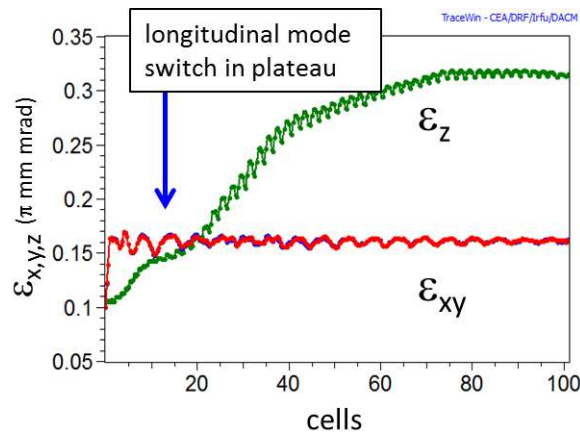


Figure 2: Rms emittances (top graph) and dynamical phase advance (centre graph) for solenoid lattice with  $k_{0,z} = 120^\circ$ ,  $k_z = 76^\circ$ . Bottom graph: Longitudinal phase space at cells 23 (left) and 103 (right)).

effect. Note that Fig. 2 suggests that the envelope growth is retarded due to the exponential nature of growth from the initial very small mismatch; obviously the envelope growth occurs earlier, if a larger initial mismatch is assumed.

### FODO LATTICE WITH RF GAPS

The result differs significantly if the periodic solenoid lattice is replaced by a FODO lattice with rf gaps in each drift as indicated in the example shown in Fig. 4.

The periodicity of the transverse focusing lattice, including the space charge force from the matched envelope with the same periodicity, determines the effective transverse force periodicity. It is traditionally assumed that due to

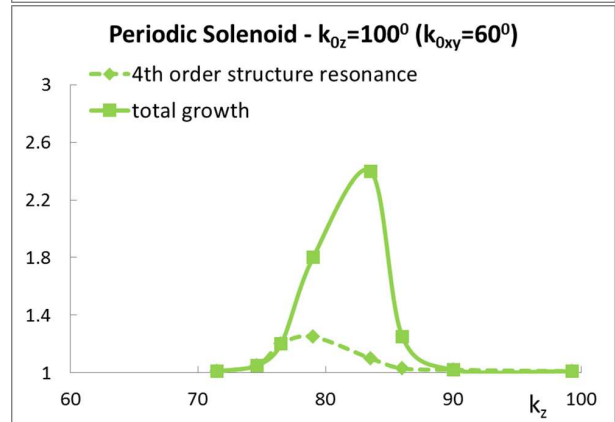
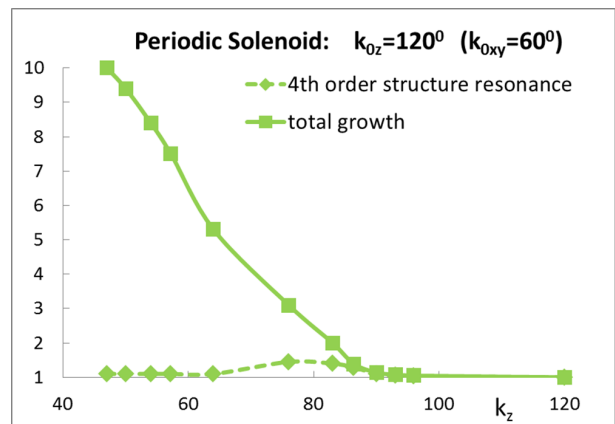


Figure 3: Complete stopband for solenoid lattice with  $k_{0,z} = 120^\circ$  (top graph) and  $k_{0,z} = 100^\circ$  (bottom graph).

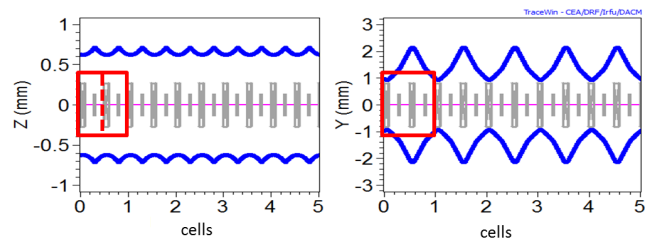


Figure 4: Example of FODO lattice with rf gaps leading to effectively halved longitudinal periods.

space charge coupling the same periodicity also applies to the longitudinal degree of freedom. We argue, however, that in the absence of space charge the relevant longitudinal period is obviously the rf period, which is half the transverse focusing period in a lattice of the kind in Fig. 4. Including space charge of a *well-matched* beam this is still approximately valid: the longitudinal space charge force of a uniform beam depends only on the transverse cross sectional area [8]. Hence, it can be assumed that it is practically identical in half-cells with focusing or with defocusing quadrupoles, and that this is also valid approximately for non-uniform beams. Thus, the effective longitudinal force periodicity even with space charge can be assumed to be given by the rf period, over which length the effective phase advance is only half as large as over the transverse focusing period.

In Fig. 5 we show the simulation results for this lattice and the same parameters as in the solenoid example ( $k_{0,z} = 120^\circ$ ) and confirm absence of any emittance growth effect, hence no  $90^\circ$  stopband. Note that the initial jump of rms emittances is due to “nonlinear field energy” effects [8]. Actually, this

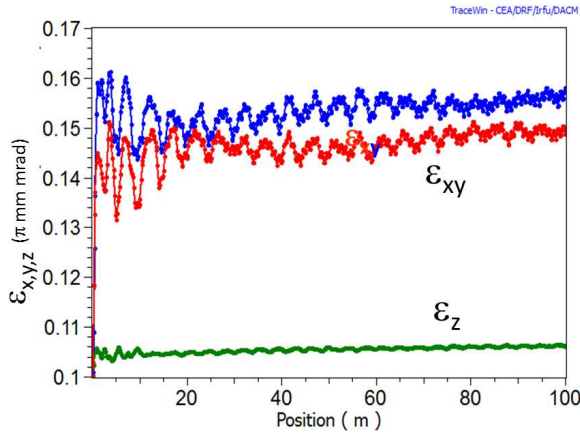


Figure 5: Rms emittances for FODO and rf gap lattice with  $k_{0,z} = 120^\circ$ ,  $k_z = 76^\circ$ .

stopband has migrated to twice as large values of  $k_{0,z}$  and  $k_z$  as a consequence of the halved longitudinal period. We note that the same migration also includes the accompanying structural fourth order space charge resonance, which always accompanies the envelope mode [4].

### SUM ENVELOPE INSTABILITY LIMIT

The next question is whether the absence of the  $90^\circ$  stopband means complete freedom of choosing  $k_{0,z} > 90^\circ$ . This is not the case due to the existence of a “sum envelope” criterion as was shown in Ref. [6].

In this context it is first helpful to remind that the conventional  $90^\circ$  envelope instability is a 1:2 parametric resonance, where the envelope eigenmode oscillates at half the frequency of the periodically varying focusing (including space charge). One can thus approximate the parametric envelope instability condition - for example in the  $xy$ -planes - by using a smooth approximation formula, which describes approximately the shift of the centre of the stopband [9]:

$$\omega \equiv 2k_{0,xy} - \Delta k_{2,coh} = \frac{1}{2}360^\circ. \quad (1)$$

Here  $\omega$  stands for the second order envelope mode “frequency” ( $= 2k_{0,xy}$  for vanishing space charge) and  $\Delta k_{2,coh}$  ( $> 0$ ) for its shift due to the coherent action of space charge. The factor  $\frac{1}{2}$  is characteristic for the parametric nature and absent if lattice driven resonances were considered (all in units of degrees per focusing lattice period).

Analogous to the conventional  $90^\circ$  envelope instability in a single plane the presence of space charge coupling between different degrees of freedom can lead to a “sum envelope” instability between the longitudinal and transverse planes as described in Ref. [6]. The resulting *sum envelope* condition

can be written in the following way

$$\omega \equiv k_{0,z} + k_{0,x} - \Delta k_{sum,coh} = \frac{1}{2}360^\circ, \quad (2)$$

where  $\Delta k_{sum,coh}$  is a coherent sum specific tune shift comparable in size with the average value of the longitudinal and transverse incoherent space charge tune shifts.

This is demonstrated in Fig. 6 for a Gaussian beam with  $k_{0,z} = 120^\circ$  ( $k_z = 92^\circ$ ) and  $k_{0,xy} = 90^\circ$  in the above described FODO lattice with initially equal emittances. Note that the actual emittance growth is relatively steep - after a phase of exponential growth from the small initial noise level. The phase space plots indicate the second order nature of the instability.

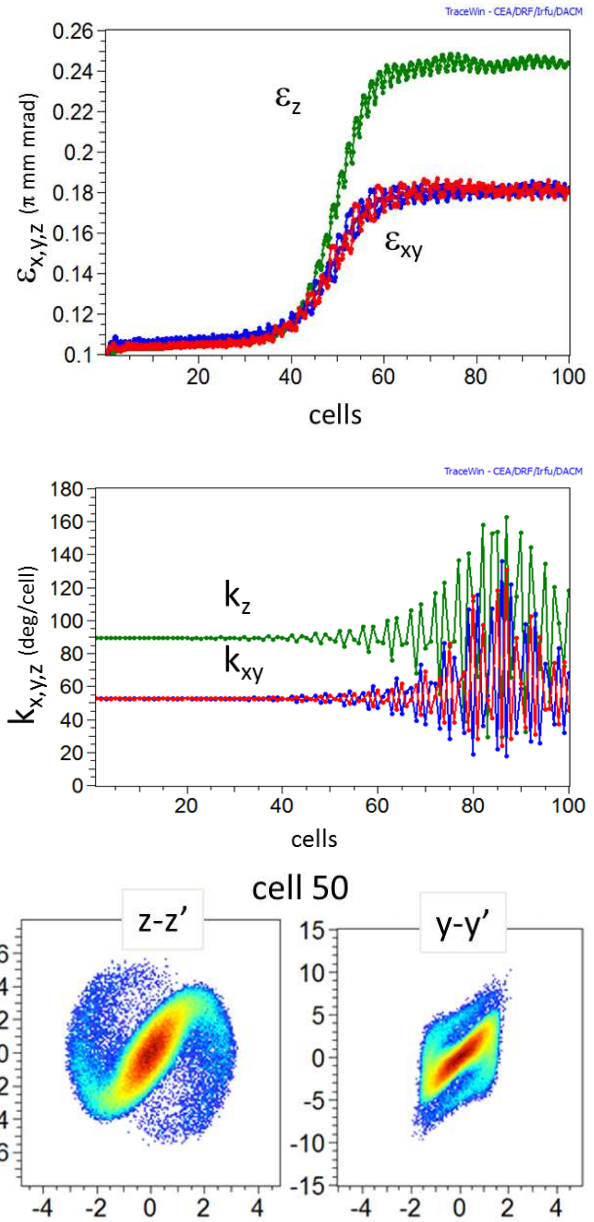


Figure 6: Sum envelope instability in FODO and rf gap lattice with  $k_{0,z} = 120^\circ$  and  $k_{0,xy} = 90^\circ$  showing rms emittances, phase advances and phase space plots.

Content from this work may be used under the terms of the CC BY 3.0 licence (© 2018). Any distribution of this work must maintain attribution to the author(s), title of the work, publisher, and DOI.

A characteristic feature is the synchronous development of emittances and envelopes in the coupled planes. Note that  $z$  couples with both,  $x$  and  $y$ , if phase advances as well as emittances in  $x$  and  $y$  are close to each other as is the case here. Thus, the growth of  $\epsilon_z$  is close to  $\epsilon_x + \epsilon_y$ .

For completeness we mention that the coherent *sum parametric* mode discussed here is essentially distinct from the well-known *single particle sum resonances* in a coupled lattice with skew quadrupoles. In the latter the coupling is external and not by a collective space charge force, besides the absence of the 1:2 parametric feature expressed by the factor  $\frac{1}{2}$  in Eq. (2) [10].

## OVERVIEW CHART

Our findings are summarized in the schematic chart of Fig. 7 valid for a lattice with halved longitudinal period as in Fig. 4. Indicated are stopbands of second (envelope) and third order parametric effects – structural resonances (see also Refs. [4, 9]) – as well as the resulting extended design region. The positive diagonal is indicating the “main 2:2 resonance” responsible for emittance exchange.

The  $xy - z$  sum envelope instability driven by the transverse lattice periodicity is described by the negative diagonal following the parametric sum rule of Eq. (2). Note that all stopbands are schematically shifted (to larger values of  $k_{0,z}$ ) to take into account the finite space charge effects, and assuming a moderate (fixed) value of space charge tune depression. The transverse envelope instability (combined with the fourth order space charge structure resonance) is associated with  $90^\circ$  following Eq. (1). For the longitudinal plane the usually assumed limit of  $k_{0,z} < 90^\circ$  is replaced by the more extended triangular region extending up to  $k_{0,z} < 180^\circ$ . Likewise, the longitudinal fourth order space charge structure resonance competing with the envelope instability in the same stopband undergoes the same movement.

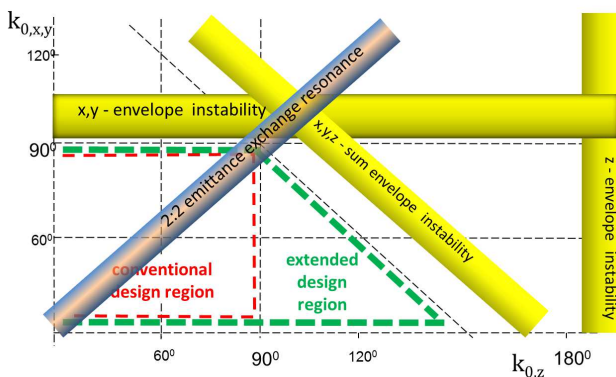


Figure 7: Schematic stability chart in the longitudinal-transverse plane for a lattice with two rf gaps per transverse focusing period, showing the extended design region (dashed green border).

## SUMMARY

In summary, the effectively shortened period in the longitudinal direction for FODO-type lattices helps to enlarge

significantly the usable area of longitudinal phase advances beyond  $90^\circ$ . It is shown that a new upper limit exists, which is given by the sum envelope instability stopband. In practical terms the sum envelope limit can be relaxed if the transverse phase advance is lowered. Detailed studies are needed to verify to what extent specific lattices, where the strict longitudinal periodicity is significantly interrupted, can still benefit from the enlargement of the usable area beyond the longitudinal  $90^\circ$ . Such deviations from strict periodicity could be, for example, due to missing cavities between cryomodules. Beam dynamics risks as well as safety of superconducting cavity operation must be balanced against desirable hardware and cost savings. Furthermore, it appears that in many cases replacing quadrupole focussing by solenoids - for the sake of creating shorter longitudinal periods - is no longer necessary.

## REFERENCES

- [1] J. Struckmeier and M. Reiser, “Theoretical studies of envelope oscillations and instabilities of mismatched intense charged-particle beams in periodic focusing channels”, *Part. Accel.*, vol. 14, pp. 227–260, 1984.
- [2] M. G. Tiefenback and D. Keefe, “Measurements of Stability Limits for a Space-Charge-Dominated Ion Beam in a Long a. G. Transport Channel”, *IEEE Trans. Nucl. Sci.*, vol. 32, pp. 2483–2485, 1985, doi:10.1109/TNS.1985.4333954
- [3] L. Groening *et al.*, “Experimental Evidence of the  $90^\circ$  Stop Band in the GSI UNILAC”, *Phys. Rev. Lett.*, vol. 102, pp.234801, 2009, doi:10.1103/PhysRevLett.102.234801
- [4] I. Hofmann and O. Boine-Frankenheim, “Space-Charge Structural Instabilities and Resonances in High-Intensity Beams”, *Phys. Rev. Lett.*, vol. 115, pp. 204802, 2015, doi:10.1103/PhysRevLett.115.204802
- [5] I. Hofmann, “Coherent Parametric Instabilities”, in *Space Charge Physics for Particle Accelerators*, Springer, New York, 2017, chapter 7, pp. 81–113.
- [6] I. Hofmann and O. Boine-Frankenheim, “Dispersion-Induced Beam Instability in Circular Accelerators”, *Phys. Rev. Lett.*, vol. 118, pp. 154801, 2017, doi:10.1103/PhysRevLett.118.154801
- [7] D. Uriot and N. Pichoff, “Status of TraceWin Code”, in *Proc. IPAC’15*, Richmond, VA, USA, May 2015, pp. 92–94, doi:10.18429/JACoW-IPAC2015-MOPWA008
- [8] Thomas P. Wangler, *RF Linear Accelerators*, Second Edition, Wiley-VCH, 2008, doi:10.1002/9783527623426
- [9] I. Hofmann and O. Boine-Frankenheim, “Parametric instabilities in 3D periodically focused beams with space charge”, *Phys. Rev. Accel. Beams*, vol. 20, pp. 014202, 2017, doi:10.1103/PhysRevAccelBeams.20.014202
- [10] O. Boine-Frankenheim, I. Hofmann, and J. Struckmeier, “Parametric sum envelope instability of periodically focused intense beams”, *Physics of Plasmas*, vol. 23, no. 9, pp. 090705, 2016, doi:10.1063/1.4963851